Volume 1 | Number 1 | Jan 2013 | Pages 1–100

Journal of
Materials Chemistry B

Materials for biology and medicine
www.rsc.org/materialsB

ROYAL SOCIETY
OF CHEMISTRY

ROYAL SOCIETY
OF CHEMISTRY

www.rsc.org/materialsB

Mimicking Natural Cell Environments: Design, Fabrication and Application of Bio-Chemical Gradients on Polymeric Biomaterial Substrates

Edmondo M. Benetti[a,c], Michel Klein Gunnewiek[a], Clemens A. van Blitterswijk[b], G. Julius Vancso[a], Lorenzo Moroni[b]

Gradients of biomolecules on synthetic, solid substrates can efficiently mimic the natural, graded variation of properties by the extracellular matrix (ECM). Such gradients represent accessible study boards for the understanding of cellular activities, and they also provide functional supports for tissue engineering (TE). This review describes the most relevant methods to produce 2-dimensional (2D) as well as 3-dimensional (3D) gradient supports for cell manipulations, and also addresses the response of cells from different origins when seeded on these constructs. The fabrication strategies summarized encompass the combination of polymer and surface chemistry, micro- and nano-engineering construction strategies and biotechnological approaches. This multidisciplinary scheme has enabled the design and the realization of diverse, synthetic supports as cellular environments, spanning from the first gradient self-assembled monolayer (SAM) to multilayers, and hybrid constructs mimicking the complexity of natural tissue environments. The standing challenge is bringing these advances in supports' fabrication to a dynamic functioning in space and time, towards the successful imitation of the most complex bio-chemical system ever studied: our body.

Introduction

Current research activities in the development of polymeric biomaterials are progressing towards the design of two-dimensional (2D) and three-dimensional (3D) supports presenting a gradual variation of biochemical composition and/or physico-chemical properties. This trend is principally driven by the need of closely mimicking the natural variation of extra-cellular matrix (ECM) characteristics including spatial definition of the behavior of seeded cells on the synthetic supports.[1, 2] Scaffolds of various compositions and presenting gradient properties have the capability of triggering several biological processes like cell migration via haptotaxis[3] and durotaxis[4]. Alternatively, gradient-containing supports can be applied to closely reproduce the physical properties of the natural tissue counterparts, simultaneously hosting tissue-(re)forming cells, like in the case of gradient hydrogel supports replacing damaged parts of bone-cartilage joints.[1, 5]

In both these cases, the engineering and fabrication of synthetic ECMs encompass the spatial variation of at least one support's characteristic, either chemical (e.g. protein concentration[6, 7] or hydrophilicity[8]), physical (e.g. matrix stiffness[9]) or morphological (porosity[10]).

The design of 2D platforms presenting bio-chemical gradients have largely relied on the controlled surface deposition of proteins by physisorption or covalent attachment, and often included the application of (macro)molecular "spacers", such as self-assembled monolayers (SAMs) or polymer brushes on inorganic surfaces.[2, 11] In contrast, 3D supports featuring

gradient compositions [12-14] have been mainly fabricated starting from hydrogel materials, using poly(ethylene glycol) (PEG) derivatives, for instance, and decorating the synthetic matrix with biomolecules or specific cellular cues via controlled loading. [14, 15, 16, 17] Additionally, 3D porous scaffolds for TE formulations have been developed by a number of diverse fabrications, to yield controlled and gradual variations of macro, micro and nanoporosities. The so-created morphological gradients regulated the settlement of cells, the diffusion of nutrients and the removal of cellular waste products during cell proliferation and differentiation, also providing a progressive variation of mechanical properties within the whole support.[18-22]

In this review, we firstly focus on the most relevant strategies to synthesize 2D gradients, concentrating on the applications of polymer adlayers and brushes to trigger the controlled surface functionalization of various biomolecules. Secondly, we report the latest advances in engineering and fabricating 3D hydrogel and porous supports presenting gradients of composition and/or physical properties. The application of both 2D and 3D constructs for studying the response of cells from different origins and for the support-mediated regeneration of tissues is finally reported.

2D Protein Gradients Supported by SAMs and Polymer Brushes

The first example of an unidirectional chemical gradient on a silicon oxide surface was presented in 1992 by Chaudhury and Whitesides, who exploited vapour deposition of different silane-based adsorbates to create SAMs featuring gradient-like surface concentrations of hydrophobic species.[23] Inspired by these pioneering fabrications, several mixed SAM compositions were subsequently employed as platforms for the formation of surface gradients of adsorbed proteins on gold substrates. For instance, Tirrell et al. reported the

a. Department of Materials Science and Technology of Polymers, MESA+ Institute for Nanotechnology, University of Twente, P.O. Box 217, 7500 AE Enschede, The Netherlands, E-mail: edmondo.benetti@mat.ethz.ch
b. Department of Complex Tissue Regeneration, MERLN Institute for Technology Inspired Regenerative Medicine, Maastricht University, P.O. Box 616, 6200 MD Maastricht, The Netherlands
c. Laboratory for Surface Science and Technology (LSST), Department of Materials, ETH Zürich, Vladimir-Prelog-Weg 5, CH-8093 Zürich, Switzerland

This journal is © The Royal Society of Chemistry 20xx

J. Mater. Chem. B, 2015, 00, 1-3 | 1

preparation of a surface concentration gradient of hydrophobic, protein-adhesive thiol species. By this method, a first SAM was uniformly deposited on Au, followed by the electrochemistry-assisted desorption of the constituting thiol species, which could be spatially controlled through the application of a decaying potential window across the functionalized substrate.[24] The so-obtained surface gradient of thiol coverage was subsequently "back-filled" with biopassive, oligoethylene glycol-bearing thiols, finally yielding a gradual variation of the bio-adhesive character across the surface.[24-27] On this SAM, protein adsorption could be spatially controlled along the gradient, enabling the fabrication of a unidirectional variation of protein surface density.[28, 29]

More recently, Bonifazi et al.[30] fabricated gradients of SAMs by varying the exposure time of single Au substrates in solution mixtures of peptide-exposing thiol ligands, featuring the cell-migration stimulating factor Ile-Gly-Asp-Gln (IGDQ), and bio-inert thiol species.[31] The so-formed gradient mixed monolayers were subsequently applied to investigate the migratory behavior of metastatic breast cancer cells compared to human dermal fibroblasts. An individual rather than a collective cancer cell migration was thus highlighted, suggesting the coexistence of "stationary" and "migrating" cell phenotypes.

SAMs presenting a gradual variation of chemical composition on silicon oxide and gold substrates were also applied for the subsequent surface-initiated polymerization (SIP) to form polymer-brush, grafting-density gradients (Figure 1).[32-36] The fabrication of these polymeric supports typically relied on the preliminary formation of a SAM of initiator adsorbates presenting a gradient coverage across a single substrate (Figure 1a). Subsequent SIP (Figure 1b) produced a graded variation of polymer grafting density along the sample, obtaining layers of grafts progressively shifting their conformation from low-density mushrooms towards high-density brushes (Figure 1c).[37-39]

Similar polymer brush platforms were successfully employed to study protein and cell adhesion, and to dissect the influence of brush-design parameters on bio-adhesion.[40-45] A relevant example was provided by poly(2-hydroxyethyl methacrylate) (PHEMA) grafts presenting a gradual variation of grafting densities and chain lengths, which were extensively applied as biointerfaces by the group of Genzer.[46, 47] Orthogonal double gradients of both PHEMA grafting density and brush molar mass were fabricated by applying mixed initiator SAMs showing a gradual variation of initiator coverages along one substrate direction, coupled with a progressive increase in the applied polymerization time (by varying substrate-polymerization solution contact time) (Figure 1d) along the direction orthogonal to the first gradient. The so-created brush platforms were subsequently incubated in fibronectin (FN) solutions, demonstrating how thick and dense PHEMA brushes significantly inhibited the adsorption of this protein, while, for a given grafted chain-length, a progressive increase of adsorbed FN could be obtained by gradually decreasing the grafting density of PHEMA films. Hence, the PHEMA brush orthogonal gradients translated into surface gradients of physisorbed FN and were finally tested for monitoring the

adhesion of MCT3T-E1 cells, which promptly responded to the bi-directional variation of surface coverage by adhesive cues, displaying a progressive change of cell number and spreading area along the substrate.

The functionalization of biomaterial surfaces by grafted-from, gradient polymer brushes has been not only devoted to study and prevent the adsorption of proteins, but also to create cell-adhesive interfaces, which can trigger in a spatially-defined way specific cellular responses. Thickness gradients of thermoresponsive poly-N-(isopropylacrylamide) (PNIPAM) brushes, fabricated following the Genzer's method, were applied for studying the adhesion of human liver cancer cells (HepG2) above the lower critical solution temperature (LCST) of PNIPAM, and their subsequent detachment below LCST.[48] The so-fabricated gradient brushes allowed a spatial modulation of the reversibility of cell adhesion. Namely, for a specific range of PNIPAM brush thicknesses across the gradient, HepG2 cells were shown to promptly adhere at temperatures above 37°C, and nearly quantitatively detach at 24°C.
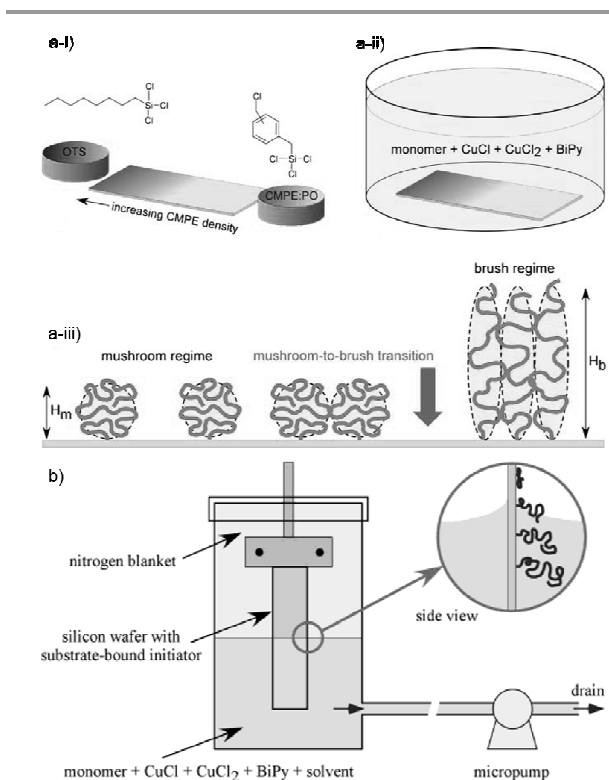

Figure 1. (a) Preparation of a SIP initiator gradient by controlled deposition on silicon oxide surfaces. (b) Surface-grafted polymer brushes presenting a gradient in grafting densities are subsequently formed by SI-ATRP. (c) Schematic illustrating grafted polymer conformations in the mushroom and brush regimes, and the mushroom-to-brush transition. Adapted with permission of Springer, reference [49]. (d) Schematic of the setup for the fabrication of surface grafted polymer brushes with a gradient in molecular weight. Adapted with permission from reference [50]. Copyright 2003 American Chemical Society.

2 | J. Mater. Chem. B, 2015, 00, 1-3

This journal is © The Royal Society of Chemistry 20xx

The application of polymer brush gradients for tuning cell attachment was recently investigated by the groups of Benetti, Vancso and Moroni, which fabricated poly(oligoethylene glycol)methacrylate (POEGMA) brush platforms presenting a gradual variation of tethered-chain length (brush thickness) and bearing cell-adhesive FN units to regulate the mechanisms of settlement by human mesenchymal stem cells (hMSCs).[51]

In this study, the variation of POEGMA brush thickness within the 10-60 nm range along a single substrate was achieved by surface-initiated atom transfer radical polymerization (SI-ATRP) from initiator-functionalized poly-ε-caprolactone (PCL) surfaces, and by gradually varying the exposure time of the initiating substrates to the polymerization medium. Subsequent functionalization of the POEGMA brushes by FN, produced cell-adhesive platforms presenting constant protein coverage, grafting density and solvent content but also displaying a progressive variation of brush-tether length. This translated into a gradient of frictional dissipation and brush lateral deformability along the surface, where thicker brushes could be more laterally deformed and showed higher friction, as measured by lateral force microscopy (LFM), while thinner ones showed reduced shear deformability and lower frictional dissipation. The gradual variation of these properties was demonstrated to alter the adhesion and spreading of hMSCs, which responded to the modulation of the dissipative character by POEGMA-FN adducts. Following a direct relationship, hMSCs area progressively decreased with the increasing of POEGMA brush lateral deformability (expressed as maximum brush lateral strain), indicating that the dissipative character of brush-cue adducts and cell spreading are synergistically correlated.[52-55] The different strengths of cell adhesion along the brush gradient were also reflected by a variation of the morphology and distribution of focal adhesion complexes (FAs) across the cell membranes.

As displayed in Figure 2, on thinner brushes larger and oriented FAs were delocalized over the whole cell membrane. With increasing brush thickness, smaller FAs were increasingly concentrated at the periphery of the membrane. Hence, a gradual variation of brush parameters was demonstrated to regulate the adhesion and spreading of stem cells. These findings additionally suggested that brush gradients could be effectively applied in more complex preparations with the aim of directing cell proliferation and, ultimately, differentiation. Following an alternative preparation of brush films, based on a grafting-to method, the group of Spencer applied poly(L-lysine)-graft-PEG graft-copolymers (PLL-g-PEG) to form thin PEG-brush layers on titanium oxide (TiO_2) surfaces.[56] Due to the electrostatic interactions between the positively charged PLL backbones and the negatively charged TiO_2 surface, and by varying the exposure time of the adsorbing polymer solutions along the substrate, a gradient in surface density of adsorbed copolymer was easily obtained. This translated into a gradual variation of PEG surface density, which was expressed as concentration of EG-units across the formed gradient, ranging from 0 to around 17 EG-units·nm^{-2}. These platforms were subsequently applied to spatially control the adsorption of bovine serum albumin (BSA) and fibrinogen (Fgn).[57] Although the adsorption of both these proteins gradually decreased with increasing EG density, quantitative inhibition of Fgn adsorption required higher PEG coverage (EG-units=12.8 ± 0.6 nm^{-2}) compared to BSA (EG-units=8.3 ± 0.8 nm^{-2}). These differences in adsorption behavior between BSA and Fgn were attributed to the lower energy cost for Fgn to adhere between PEG chains (or on film defects), provided by the distinctive morphology of this coil-like protein, capable of undergoing secondary adsorption on too thin or not uniform brush films.[58] The remarkable advantage of this brush gradient fabrication strategy, compared to the already reported grafting-from methods, is represented by its easy and reproducible dip-and-rinse process and the possibility to coat large surfaces in a controlled fashion. Additionally, structured PLL-g-PEG films can be applied not only on metal oxide surfaces but also on glass and silicon oxide substrates.[59, 60]

Microfluidic- Assisted Fabrication of 2D Gradients on Hydrogel Substrates

As hydrogel supports has been often applied as highly versatile platforms for regulating the settlement of cells and studying their behavior in response to chemical or physical stimuli,[61, 62] the surface engineering of these substrates has progressively gained increasing impact in the development of biomaterials. Novel surface modification/functionalization strategies exploiting microfluidic devices to deposit (bio)chemical species in a spatially controlled fashion have recently emerged as powerful alternatives compared to the commonly applied "static" solution treatments.

Particularly, the formation of lamellar flows of protein solutions inside microchannels[63, 64] was successfully applied to physically or chemically deposit proteins and other
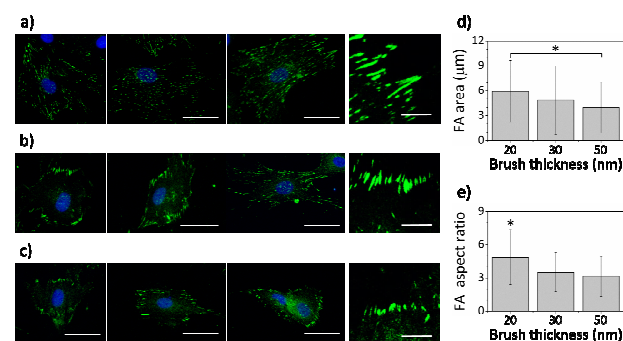

Figure 2. Immunofluorescence micrographs showing the vinculin-associated FA complexes for hMSCs attached on 10-20 (a), 30-40 (b) and 50-60 (c) nm-thick POEGMA brushes functionalized with FN. The FA points were stained by FITC (green) and the cell nucleus by DAPI (blue). (d) Average FA area and (e) average FA aspect ratio. * denotes statistical significant differences between the assigned and the non-assigned topographies (p < 0.05). Adapted with permission from reference [51]. Copyright 2015 Wiley-VCH Verlag GmbH & Co.

biomolecules onto hydrogel surfaces placed in contact with the flow (Figure 3a,b).[63-67] Gradient of adsorbed proteins on poly(dimethylsiloxane) (PDMS) substrates were similarly fabricated by exploiting the progressive depletion of protein concentration in the fluid channel,[63, 68] which finally yielded surface concentration gradients of biomolecules with typical extensions ranging from sub-micrometer to several centimetres in lengths (Figure 3c).[69] Following a similar approach, yet employing multichannel devices, patterns of different proteins could be formed, finally obtaining multiple gradient arrays and double gradients featuring two different protein species on glass supports, as shown in Figure 3d.[68]

Protein gradients on hydrogels can be fabricated also along the width of microchannels by injecting two or more protein solutions into a fluidic-based system composed of alternated splitting and mixing units.[64, 70, 71] When two inlets were used, one containing a protein solution and the second just a buffer solution, a single gradient of one protein was formed between the walls. Alternatively, the addition of a solution of a second protein through an additional inlet allowed the fabrication of hydrogels featuring concentration gradients of two different proteins.[72] The designing of microfluidic devices presenting three or more inlets additionally enabled the fabrication of more complex, multiple-protein concentration profiles.[64]

Figure 4. (a) A microfluidic chip used for hydrodynamic flow focusing. Fluorescence micrographs and graphical representations obtained by image analysis of a (b) linear, (c) exponential and (d) Gaussian gradients of FITC-BSA-Biotin on NeutrAdvidin-conjugated PEG gels (scale bar = 100 mm). Adapted from reference [73] with permission of The Royal Society of Chemistry.
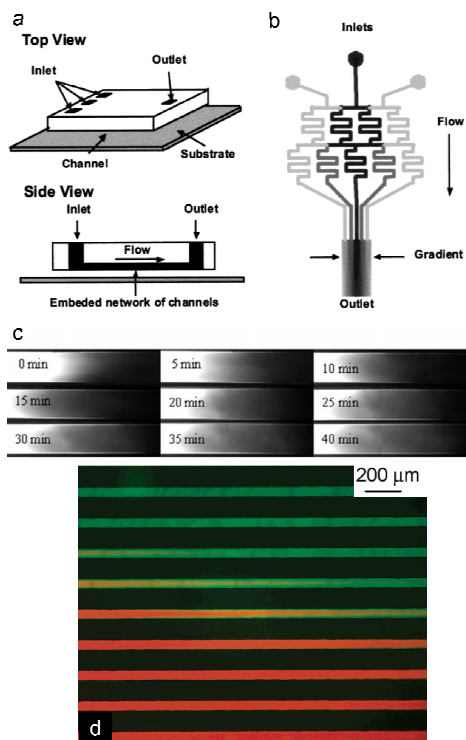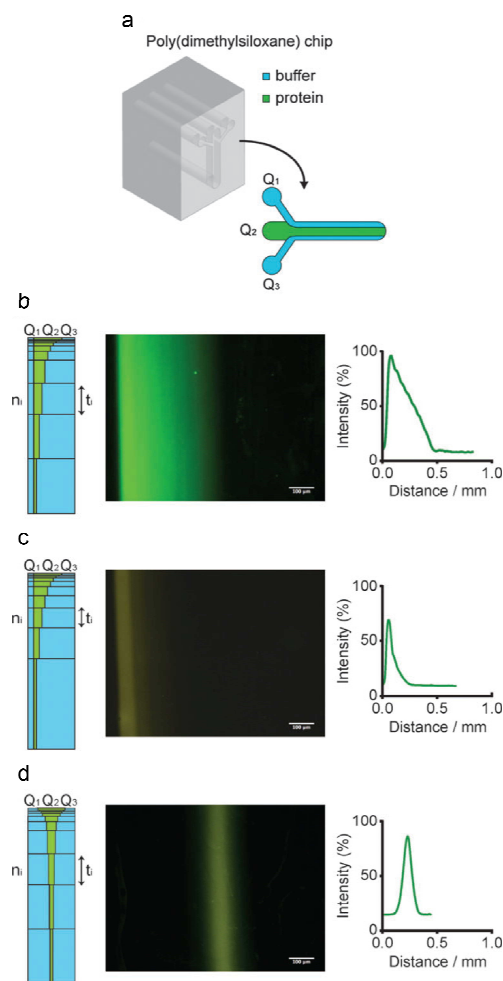

Figure 3. (a) A microfluidic gradient generator setup and (b) a schematic design of a gradient-generating microfluidic network using three inlets. Adapted with permission from reference [64]. Copyright 2000 American Chemical Society.. (c) Fluorescence micrographs depicting an example of the fabricated gradients at different backward-flow times. Adapted with permission from reference [69]. Copyright 2010 Wiley-VCH Verlag GmbH & Co. (d) Counter-propagating gradient of BSA (orange-red) and collagen (green) with pre-exposure of PDMS to BSA. Adapted with permission from reference [68]. Copyright 2003 American Chemical Society.

Another gradient fabrication technique based on microfluidics was introduced by the group of Lutolf, which exploited hydrodynamic flow focusing (HFF) to create protein gradients on PEG-hydrogel surfaces through protein-specific binding functions (Figure 4a).[73] In this method, NeutrAvidin-decorated PEG-hydrogels were functionalized by different biotinylated biomolecules flowing through a microchannel system presenting three independently controlled inlets.

The composition and the morphology of the subsequently formed surface gradients could be efficiently controlled by adjusting the flow rates in the individual channels, which also determined the width and the position of the different protein solution streams (Figure 4b-d).[73, 74]

The above-mentioned fabrications relied on the variations of surface exposure times by one or more protein solution streams. Alternatively, a gradual modulation of protein concentration within a flow, coupled with the application of diverse protein media via multiple injection steps, was

4 | J. Mater. Chem. B, 2015, 00, 1-3

This journal is © The Royal Society of Chemistry 20xx

employed to design complex protein patterns and gradients on similar hydrogel surfaces.[75] [73-75]

This fabrication strategy was experimented by the same research group of Lutolf, which created patterns of four parallel, linear gradients of fluorescently-labelled human immunoglobulin (hIgG) with micrometer precision on PEG gel substrates (Figure 5a,b). Following a first solution flow-assisted deposition, the simple rotation of the pre-functionalized chip by 90° (Figure 5c) allowed the formation of four additional micropatterns of BSA-biotin concentration gradients, finally obtaining an array of orthogonally intersecting gradient patterns (Figure 5d,e).
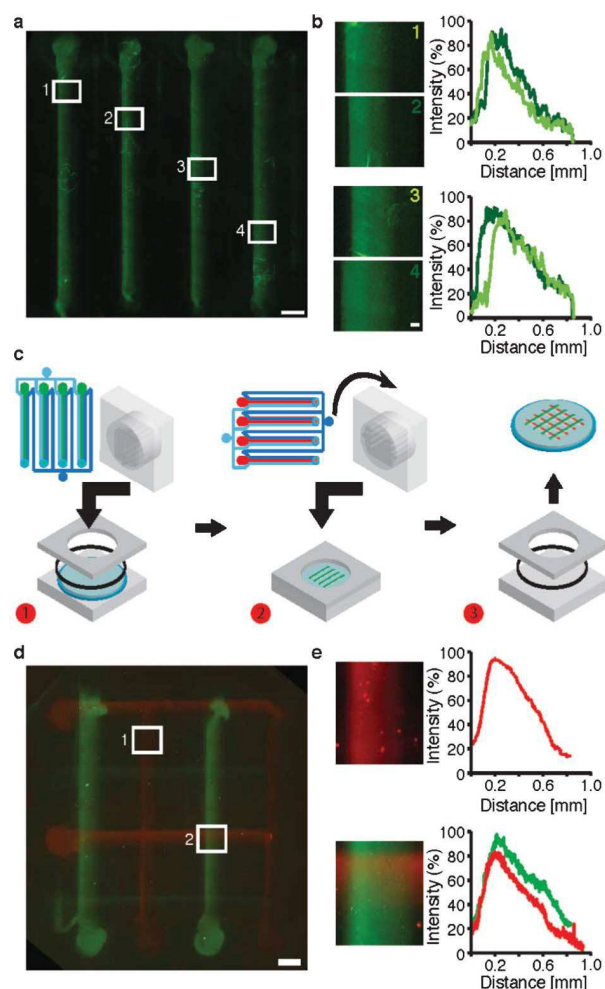

Figure 5. (a) Stitched micrographs of a pattern of four parallel arrayed protein gradients. (b) Micrographs showing the magnification of individual gradients (white frames) and a graphical representation of their respective intensity profiles (scale bar = 100 mm). (c) Patterning of arrays presenting overlapping gradients. Step 1: The microfluidic device is assembled and the first set of four gradients is patterned. Step 2: the microfluidic device is partially disassembled with the patterned hydrogel remaining fixed to ensure good alignment. The microfluidic chip is turned by 90° and the second set of parallel gradients is deposited. Step 3: the patterned hydrogel is recovered. (d) Stitched micrographs of a four-by-four gradient array of two different proteins. (Scale bar = 900 mm). (e) Micrographs of regions of interest of the gradient array (white frames) and a graphical representation of the corresponding intensity profiles. Reproduced from reference [74] with permission of The Royal Society of Chemistry.

The application of microfluidic techniques to create surface-gradients of biomolecules demonstrated a highly powerful and versatile engineering approach to structure with high precision and reproducibility a variety of hydrogel and elastomeric substrates. These attracting advantages unfortunately suffered from some limitations, mainly related to the impossibility to structure areas on substrates larger than few centimetres.

This drawback restricted the applicability of such methods to design study-platforms for addressing isolated biological phenomena without having the capability of scaling-up these fabrications for the structuring of macroscopic supports for TE. In the following paragraph, alternative fabrications for producing gradient supports from 2D to 3D that can be extended to build large scaffolds maintaining very high feature resolutions are presented.

3D Gradients on Porous Scaffolds

The increasing applications of porous scaffolds in TE formulations stimulated the development of fabrication/surface modification methods allowing the formation of 3D (bio)chemical gradients within these supports. The large majority of the most advanced methods to create 3D gradients on porous scaffolds directly derived from analogous surface functionalization strategies applied for flat surfaces, additionally expanding substrate structuring in the third dimension or coupling controlled, layer-by-layer depositions of single constituents to finally yield three-dimensional constructs. This is the case of electrospinning,[22] a well-known process to fabricate porous constructs. In this method, the application of a high voltage is exploited to create an electrically charged flow of a polymer solution or a polymer melt from a nozzle to a collector plate.[76] As the polymer solidifies, it forms an interconnected porous web of fibers. Electrospun constructs featuring gradient chemistries and/or physical properties have been manufactured by gradually varying the composition of the electrospinning solution at a single nozzle. This strategy was explored by applying several different setups, which basically exploited the same principle of progressive mixing of electrospinning feeds. These included the "gradient maker",[77] a microfluidic device dispensing polymer solutions with varying compositions[78] or, alternatively, a setup where two polymer solutions mix in different proportions at a T-junction.[79]

Compositional gradients of electrospun fiber mats could be also obtained by a double electrospinning process, as exemplarily shown in Figure 6.[80] In this case two spinnerets were placed at the opposite side of a rotating drum and the flow rate of both solutions was varied independently.[81, 82] Keeping steady the collector plate or the rotating drum at a certain position, a compositional gradient along the vertical axis of the construct was successfully fabricated. Additional lateral movement of the spinneret along the drum allowed the formation of an additional gradient of fiber composition along the horizontal axis of the scaffold.[83, 84]
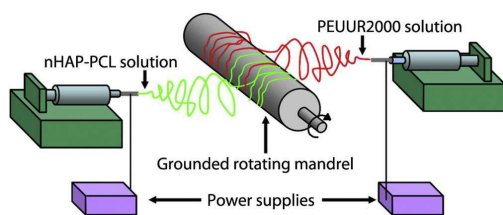
This journal is © The Royal Society of Chemistry 20xx

J. Mater. Chem. B, 2015, **00**, 1-3 | **5**

Figure 6. Schematic illustrating an electrospinning apparatus with offset spinnerets. Reprinted from reference [80], Copyright 2011, with permission from Elsevier.

Using similar apparatuses, gradient electrospun scaffolds including different proteins incorporated within the fiber structures could be also created. The embodied biomolecules were subsequently released in the surrounding medium,[77, 78, 83, 85] or, alternatively, remained anchored to the fiber surface (via heparin-mediated linkages, as an example).[84]

Following alternative, fiber-surface functionalization strategies, the gradual diffusion of calcium phosphate[86], proteins[87], or aminolysis[88] solutions within the pre-formed electrospun polymer supports was reported to allow the chemical modification of the support according to a gradient morphology. In all these cases, due to the high porosity of the fiber mats, solutions of adsorbates or reactants could diffuse by capillarity into the support and create a unidirectional, compositional gradient throughout the 3D structure. As an example, the group of Chen applied the controlled diffusion of protein solutions within a poly(methylglutarimide) (PMGI) fiber network, successfully producing 3D gradients of physisorbed FN.[87] By additionally varying the diffusion speed as well as the FN concentration in the diffusing solutions, the efficient modulation of FN gradient coverages throughout the constructs could be achieved. In a similar way, the group of Li created a gradient of amino functions at the fibers' surface by varying the aminolysis time across the structure of a poly(DL-lactide) (PDLLA) electrospun fiber mat.[88] The exposed amino groups were subsequently coupled to gelatin units, finally forming a gradient of biomolecules within the 3D support.

Controlled diffusion of surface modifiers and/or biomolecules could be also applied to form compositional 3D gradients within microporous constructs initially obtained by other fabrications.
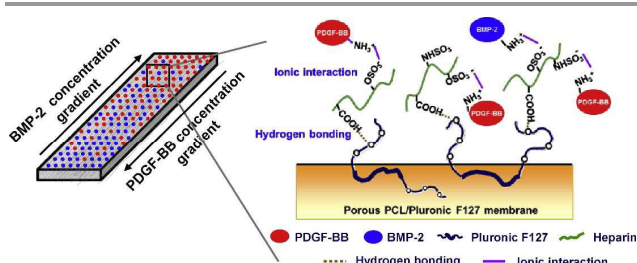

Figure 7. The formation of a PCL/Pluronic F127 membrane with reverse gradients of PDGF-BB and BMP-2, and the successive binding of heparin and growth factors onto the membrane surface. Reprinted under permission from reference [89], Copyright 2014, with permission from Elsevier.

Multidirectional gradients of two different growth factors (GFs) within microporous PCL membranes, previously obtained by an immersion/precipitation method,[90] could be formed by controlled diffusion and heparin-mediated adsorption of proteins, as demonstrated by the group of Lee (Figure 7).[89] Applying a comparable diffusion-aided functionalization strategy, scaffolds fabricated from centrifugation of PCL fibrils to form 3D structures featuring a mono-directional gradient of porosity, could be decorated with GFs via heparin-binding.[89, 91-94] An increment of surface concentration of GFs on the fiber constituents thus reflected an increase of the available surface area along the porosity gradient. This effective fabrication paved the way for possible further developments in the gradient composition (e.g. the application of multiple GFs within the same construct) or in the formation of double gradients, including both porosity and protein composition/concentration.

The fabrication of multi-directional, 3D gradients of different proteins within biodegradable scaffolds has represented a fundamental step forward to the designing of synthetic ECMs more closely mimicking the natural counterparts, and could gain an enormous impact for regenerative medicine. Pursuing this challenging objective, the groups of Benetti, Vancso and Moroni recently reported the fabrication of 3D gradient scaffolds by a combination of rapid prototyping (RP) of biodegradable thermoplastics[95, 96] and their subsequent functionalization by SI-ATRP of POEGMA (Figure 8).[97] Due to the regular microporosity of the supports, provided by RP, and the high surface energy of their exposed surface, assured by the hydrophilic POEGMA brush coatings, the diffusion of different protein solutions could be precisely controlled within the construct in a multidirectional fashion. This allowed creating radial and axial gradients of two different proteins in the same support. The application of similar controlled depositions, utilizing FN solutions within POEGMA-coated PCL scaffolds, allowed the formation of FN-based multidirectional gradients, which could spatially direct the settlement of adhering stem cells with extraordinary precision. The advantage of this fabrication method, as compared to e.g. functional hydrogel supports, is the ease of preparation and the capability of forming multiaxial gradients of proteins keeping full control over gradient characteristics and morphology.

3D Gradients within Hydrogel Supports

Despite the high potential and attractive properties of microporous thermoplastic supports, hydrogel-based constructs presenting gradient compositions are still intensively developed by numerous research groups worldwide and hold some unique features. Noteworthy, the composition of hydrogels is highly tuneable, enabling the introduction of diverse functions for protein immobilization and the tailoring of the construct biodegradability.

6 | *J. Mater. Chem. B*, 2015, **00**, 1-3

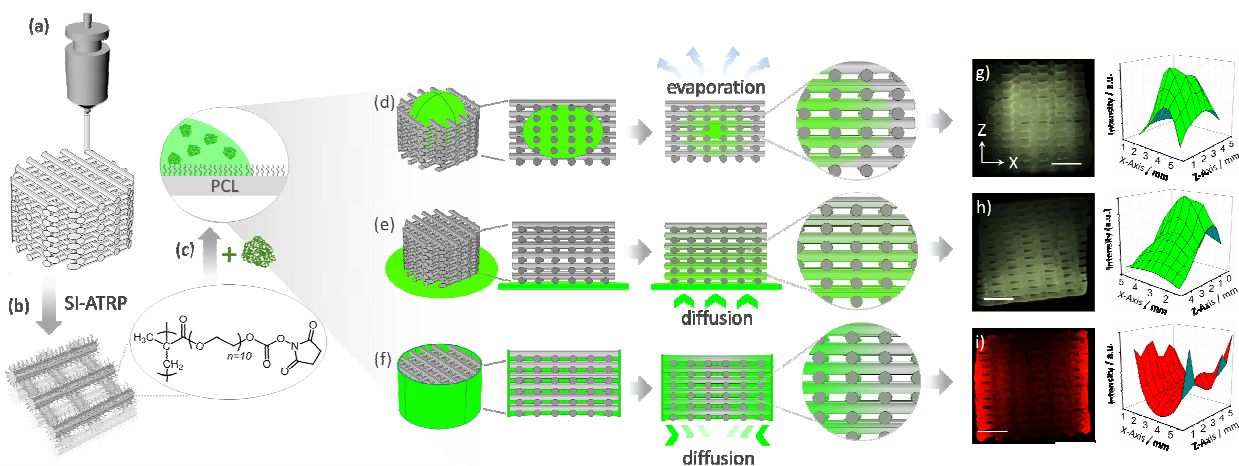This journal is © The Royal Society of Chemistry 20xx

Figure 8. POEGMA-brush-assisted fabrication of 3D protein gradients within PCL scaffolds and application as platforms for stem cells immobilization. a) Fabrication of PCL microporous scaffolds by rapid prototyping; b) SI-ATRP of OEGMA from the PCL fibers network and subsequent activation of hydroxyl side chains to form NHS esters; c) conjugation of proteins at the brush interface by controlled diffusion of solutions within the 3D scaffolds. This last step is especially highlighted in (d–f). d) Incorporation of microdroplets of protein solutions and subsequent solvent evaporation generated radial concentration gradients on brushes. e) Controlled diffusion from a soaked paper reservoir allowed the formation of axial protein concentration gradients. f) Wrapped soaked paper reservoirs enabled protein diffusion from the lateral walls of the scaffolds and the consequent fabrication of radial protein gradients developing oppositely to (d). Fluorescence micrographs and the corresponding fluorescence intensity plots of PCL–POEGMA scaffolds functionalized with gradients of BSA concentration in the (g) inside-to-outside, (h) bottom-to-top and (i) outside-to-inside directions. Adapted with permission of reference [97]. Copyright 2015 Wiley-VCH Verlag GmbH & Co.

In addition, (stem) cell preparations can be directly blended within the hydrogel matrices, during their construction, allowing the manufacturing of injectable pre-tissues in a single fabrication step. Generally, the construction of hydrogels featuring a gradual variation of composition in 3D has encompassed either (i) the deposition of pre-polymer solutions with progressively varying composition, followed by crosslinking and "fixation" of the whole matrix or (ii) the application of a physico-chemical stimulus within or on a pre-formed hydrogel matrix, capable of spatially propagating a structural or chemical modification of the support along one or multiple directions. In the first class of fabrication strategies lays the "gradient maker" technique, which has been recently developed by the group of West.[6] In this method, the controlled moulding of hydrogel precursors is accomplished by utilizing an apparatus made of two interconnected chambers that contains different pre-polymer solutions, as exemplified in Figure 9a. As the solution in chamber 1 is drained from the apparatus into a mould, it is simultaneously re-filled with the solution coming from chamber 2. While chamber 1 is continuously stirred, it is progressively diluted with the solution from chamber 2 until the outflowing material nearly reaches the composition of this last chamber. Applying photocurable hydrogel precursors and subjecting the moulded constructs to UV irradiation, a hydrogel matrix presenting a gradient composition is finally formed. This versatile technique was successfully used to gradually vary the physical properties[98, 99] as well as the chemical composition[100] of hydrogel supports in a 3D fashion (Figure 9b).

Similarly to this method, the groups of Langer and Netti applied a multichannel, microfluidic device to gradually vary RGD (Arg-Gly-Asp) concentration within a precursor PEG-based solution for hydrogel fabrication. Subsequent photocuring of

the so-formed pre-polymer mixture allowed to fix the RGD gradient across the hydrogel construct.[70, 101]

Following an analogous method, hydrogels with a 3D variation of composition could be fabricated using a multiple syringe setup.[102-104] The gradual variation of the pre-polymer solution feed from each individual syringe, followed by photocuring, enabled the fabrication of different protein concentration gradients within PEG hydrogels.

The construction of more complex architectures including organizations of cells, matrix components, and biological cues by controlled deposition of hydrogel precursors was proposed by Weber et al., who combined 3D printing with layer-by-layer patterning of diverse ECM constituents (Figure 10).[105] This process consisted of a sequential deposition of a PDMS mould containing a precursor solution, a layer of PEG hydrogel and a patterned or uniform layer consisting of a combination of cells, biomolecules and hydrogel material.
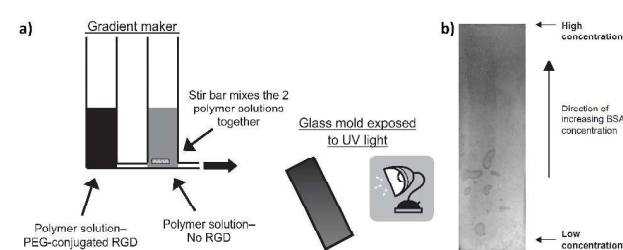
Figure 9. (a) Schematic representation of a gradient maker used to gradually vary the concentration of RGD within a PEG solution. The resulting polymer solution is pumped into a mould where it is finally photopolymerized. (b) Representative image of a BSA-gradient hydrogel stained with Coomassie brilliant blue. Staining intensity increased with increasing concentrations of BSA. Adapted from reference 6, Copyright 2005, with permission from Elsevier.

This journal is © The Royal Society of Chemistry 20xx

J. Mater. Chem. B, 2015, 00, 1-3 | 7

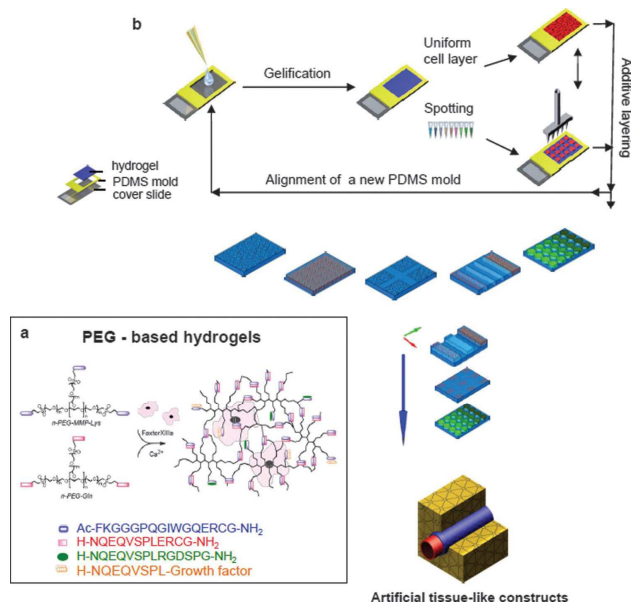Figure 10. Fabrication of the artificial tissue-like construct proposed by Weber and co-workers. (a) The components of the artificial extracellular matrix (aECM) applied for the hydrogel formulation. (b) A first layer of PEG-based hydrogel is casted with the help of a PDMS mask, then combinations of cells, biomolecules, and hydrogel are deposited as either uniform or patterned layers. By repetitive alignment of the PDMS moulds different heterogeneous designs are formed. The final layer-by-layer assembly of individually patterned layers results in a tissue-like construct. Reprinted from reference [105] with permission of The Royal Society of Chemistry.

By repeatedly depositing these components in a layer-by-layer fashion, a complex 3D construct featuring a continuous variation of bio-components and synthetic materials was finally obtained. Although sometimes expensive and often complicated, these engineering approaches allowed producing artificial constructs closely mimicking the intrinsic compositional and physical diversities of the natural ECM.

As an alternative to fabrications involving sequential depositions of pre-hydrogel mixtures, photochemical patterning was successfully applied to spatially control the composition of hydrogel matrices in 3D, throughout already formed constructs. For instance, the local photoactivation of specific chemical functions allowed the spatially controlled conjugation of different peptides or proteins within hydrogel supports. This general strategy was addressed by involving diverse chemical triggers for bioconjugation, such as radical photoinitiators,[106-109] thiol-ene couplings,[110-112] enzymatic[113] or thiol/amine-maleimide reactions.[114, 115] As an example, several works reported the fabrication of 3D gradients of RGD and different proteins, also including the formation of gradient patterns with different geometry and complexity within PEG-based hydrogels by spatially modulating the photocleavage of carbamate and chemically protected thiol groups within a pre-synthesized matrix.[116] PEG-based hydrogels presenting 3D gradients of proteins were alternatively fabricated in the group of Ehrbar by combining electrochemistry with pH-dependent enzymatic polymerization.[117]

In this process, two electrodes were immersed within a hydrogel precursor solution based on transglutaminase (TG)/PEG/protein mixtures. The subsequent application of a potential between the cathode and the anode induced a progressive pH variation across the pre-hydrogel that eventually modulated the rate of enzymatic crosslinking along the construct. This resulted in the formation of 3D gradients of protein concentration throughout the matrix, being the biomolecules incorporated within the network structure via crossslinkable linkages. Further organization of the electrodes according to specific pattern designs and the additional application of multiple protein solutions resulted in the production of hydrogel scaffolds presenting complex and multiple 3D gradients of different proteins.

Cellular Response on Gradient Supports

When cells from different origins are incubated in contact with synthetic ECMs featuring multidimensional gradients of peptides and protein cues their behavior can be markedly altered. Namely, different cellular processes including migration, proliferation and differentiation can be efficiently regulated by bio-chemical gradients.[118-120]

It is well known that cells adhere to the surrounding ECM via cellular receptors like integrins and other adhesion proteins.[121, 122] These receptors probe the ECM and trigger specific responses depending on the environment, later on determining a number of cellular mechanisms.[118, 119, 123]

When studied on 2D supports, cell adhesion significantly depends on the concentration and distribution of ligands at the surface and a critical ligand spacing was found to induce maximum cell spreading and guarantee stable attachment.[124-127] The adhesion of human foreskin fibroblasts on surface gradients of PLL-*g*-PEG-supported Fgn confirmed that a maximum of cell adhesion was found at a very specific protein spacing (47 ± 3 nm),[57] which was very close to the value initially recorded by Spatz and co-workers on RGD-nanopatterned platforms (58 nm).[125] In accordance to these findings, when the adhesion of fibroblasts was investigated on PHEMA brush-supported FN gradients, maximum values of cell adhesion and cell spreading area were recorded on areas along the gradient characterized by protein coverages of 50 and 100 ng·cm^{-2}, respectively.[41]

In addition to adhesion, the migration of cells on flat surfaces was also found very sensitive to variations of surface coverage of protein cues and cell-adhesive peptides. In 1989 Brandley and Schnaar were the first to investigate the effect of a linear and exponential gradient of RGD surface coverage on cell adhesion and migration.[128] These studies highlighted how cell migration is always taking place in the direction of higher peptide surface densities and, thus, towards areas with a more marked cell-adhesive character. In addition, steeper surface gradients of adhesive cues stimulated longer fibroblasts migrations and faster cell locomotion.[6, 101] Similarly to surface gradients of adhesive cues, a gradual variation of basic fibroblast growth factor (bFGF) concentration on PEG-RGD-based hydrogels induced mobility of vascular smooth muscle

8 | *J. Mater. Chem. B*, 2015, **00**, 1-3

This journal is © The Royal Society of Chemistry 20xx

cells (VSMCs). Specifically, VSCMs showed an aligned morphology and moved in the direction of increasing bFGF concentration.[7] In a similar way, the application of a gradient of GF concentration throughout a loosely crosslinked agarose-based hydrogel, with increasing protein concentration from the outer surface towards the core of the structure, stimulated the migration of neural precursor cells (NPCs) inside the construct. [114, 129-131]

Cells cultured within 3D supports showed different and more complex mechanisms of migration when compared to planar substrates.[132, 133] Especially within hydrogel-based ECMs the composition and concentration of biological cues in combination with the physical properties of the polymer matrix (e.g. degree of crosslinking) were found crucial parameters determining the motility of cells.[134] As an example, Kyburz et al. showed that hydrogels with low crosslink density (0.18 ± 0.02 mM) and high RGD concentration (1 mM CRGDS) allowed relatively high migration rates (17.6 ± 0.9 $\mu m \cdot h^{-1}$).[135] Alternatively, electrospun scaffolds based on poly(lactide-co-glycolide) (PLGA) and featuring a unidirectional gradient of fiber-encapsulated bFGF, directed the migration and stimulated the differentiation of mouse dermal fibroblasts in a spatially defined manner.[85] The "depth" of cell migration through the fibrous support was determined by the steepness of the concentration gradient of bFGF. Additionally, when these supports were applied in vivo, the morphology of the protein gradient within the fibers also regulated the density of the subsequently formed blood vessels (Figure 11).

Synthetic ECMs presenting different gradients of biochemical cues were also applied to spatially control the osteogenic differentiation of seeded cells within bone/cartilage implants.[136] Similar supports were designed by the group of Li, who decorated a poly(DL-lactide) (PDLLA) electrospun construct with a gradient of gelatin and hydroxyapatite (HAP). Subsequent incubation of the gradient scaffolds with pre-osteoblasts, MC-3T3 E1, demonstrated how cell viability as well as cell density could be spatially modulated according to the gradual variation of gelatin concentration.[88] In addition, both alkaline phosphatase (ALP) activity and collagen type-I expression by MC-3T3 E1 showed a similar trend, indicating that the extent of osteogenic differentiation was regulated in response of the HAP gradient across the scaffold.

Applying a similar designing concept, Zhang et al. fabricated an electrospun PLGA scaffold containing a dexamethasone (Dex) gradient within the fibrous construct by complementing the electrospinning polymer solution with a variable concentration of Dex.[78] Hence, the local variation in Dex release at different volumes within the scaffold directed the differentiation of subsequently incubated mesenchymal stem cells (MSCs) (Figure 12). At positions of higher Dex concentration across the support adipogenesis was favoured, while volumes characterized by lower Dex content displayed a tendency by MSCs to undergo osteogenic differentiation (Figure 12).
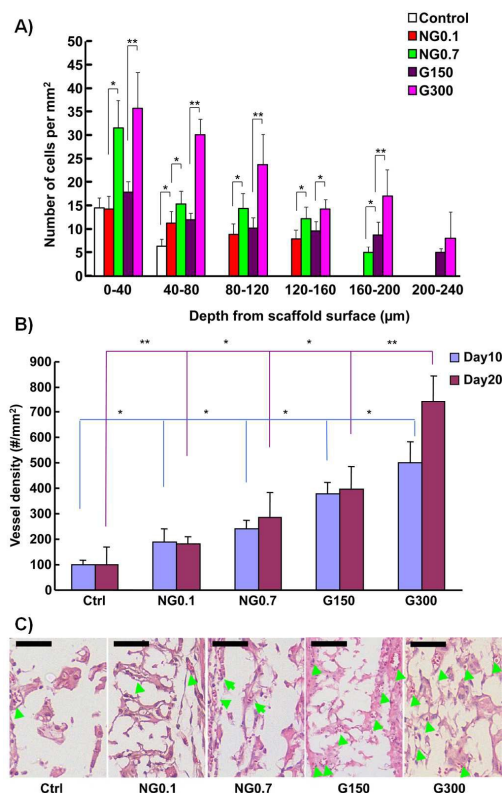

Figure 11. (A) Number of cells at different depths from the scaffold surface after 14 days of culture (*p < 0.01, **p < 0.001) quantified for NG0.1 and NG0.7 (uniform scaffolds fabricated with injection rates of 0.1 and 0.7 $ml \cdot h^{-1}$, respectively, from a 150 $\mu g \cdot ml^{-1}$ bFGF solution) and for G150 and G300 (gradient scaffolds fabricated by gradually varying the injection rate from 0.7 and 0.1 $ml \cdot h^{-1}$ from a 150 or 300 $\mu g \cdot ml^{-1}$ bFGF solution, respectively). (B) Number of vessels within the different scaffolds after 10 and 20 days of subcutaneous implantation (*p < 0.01, **p < 0.001). (C) Blood vessels within the different scaffolds after 10 days of implantation. The functional vessels that contain well-defined lumens and blood cells are indicated by green arrows. Scale bar = 50 µm. Reprinted with permission from reference [85]. Copyright 2012 American Chemical Society.

Two interpenetrating gradients of different growth factors were alternatively applied across porous PCL/pluronicF127 membranes, previously fabricated by Lee and coworkers exploiting the "diffusion method".[89] Namely, platelet-derived growth factor-b (PDGF-BB) and bone morphogenetic protein 2 (BMP-2) were deposited by heparin-mediated binding to form a double gradient of protein concentration at the exposed surface of the microporous support (Figure 14).

Adipose stem cells (ASCs) cultured within these constructs showed an upregulation of different tenogenic markers at membrane sections loaded with higher concentrations of PDGF-BB, while different osteogenic markers were progressively upregulated moving towards regions of the scaffold presenting higher concentrations of BMP-2. The spatially resolved differentiation of ASCs could be clearly recorded by the selective staining with antibodies against tenomodulin (for tenogenesis) and bone sialoprotein (osteogenesis).

This journal is © The Royal Society of Chemistry 20xx

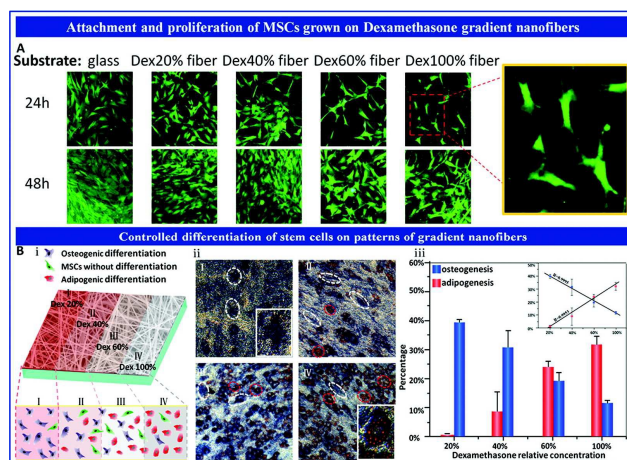*J. Mater. Chem. B*, 2015, **00**, 1-3 | **9**

Figure 12. (A) Fluorescence micrographs displaying MSC attachment and proliferation on dexamethasone gradient electrospun fibers. (B) MSC differentiation induced by the gradient substrates (i); (osteocyte) and red-oil (adipocyte) staining images of MSCs on fibers with dexamethasone concentration gradient (ii). Differentiation proportion of MSCs induced by the different gradient supports (iii). Reprinted with permission from reference [78]. Copyright 2012 American Chemical Society.

Despite more and more knowledge is available nowadays on the most optimal ligand density to promote cell adhesion, proliferation, and migration, and on biological factors availability to influence cell differentiation in 2D and in 3D systems, further studies should aim at deepening our understanding of the biological signaling pathways that are activated when material gradients are formed. On homogenous materials, cell morphology is coupled to cell function via the activation of ROCK[137] and Hippo[138] signaling, both interrelated with the underlying substrate stiffness and the consequent dynamic remodeling of cellular focal adhesions. On materials displaying gradients of physico-chemical and biological properties, little is known in terms of how these signaling pathways are activated and regulated in time. In this respect, it would be meaningful to monitor such biological processes also in time to assess long-term stability of cellular adhesion and proliferation.

A Future Perspective on Gradient Supports

Although exciting results have been obtained in translating the generation of physico-chemical gradients from 2D supports to 3D scaffolds, a few challenges remain ahead. A further control on the gradient profile would be desirable to allow the creation of biological variations that mimic more closely patterns observed in native tissues and organs. This could pass, for example, through the use and control of capillary forces where we could envision creating compartments within the same 3D volume that are predisposed to solve specific sub-functions in the targeted tissue. The further possibility to combine more chemical species in the same 3D scaffold would open the door to multiplexing, thus starting to build on the biological complexity that is needed to regenerate a fully functional tissue by mimicking the different cellular niches present in our body. The use of different polymer brushes

where different chemical end groups are present to bind different biological species combined to the generation of programmed gradients could result in the selective adhesion and activity of a heterogeneous cell population. A practical example where these strategies would be meaningful to implement is the creation of a smart scaffold that allow the regeneration of a specific tissue with the integrated vascular, neural, and lymphatic networks.

Next-generation scaffolds for cell manipulations are envisioned to be capable of dynamically triggering diverse cellular activities, simultaneously maintaining high specificity and modulating the trigger in space and time.

Generally, the already reported fabrications did not allow creating such a dynamic niche for the seeded cells. This is due to both the synthetic constituents of ECM, which must be strongly held together (covalently or physically) to host and support cells, and the (bio)chemical gradient applied on the construct, which requires to be "fixed" via an effective, fast and irreversible external stimulus (e.g. via a locally induced, prompt chemical reaction).

To overcome these limitations, the application of supramolecular building blocks to form synthetic ECMs could efficiently reproduce the dynamics of diverse cell environments. Pointing towards this challenging target, supramolecular supports for host-guest chemistries based on non-covalent interactions[139] combined with SAMs have been applied to build molecularly reversible (Figure 13)[140] and stimuli-responsive biointerfaces.[141]

Although most of supramolecular biointerfaces and biomaterials are designed to present a homogeneous distribution of functions, Jonkheijm et al. recently constructed protein gradients based on host-guest chemistries across a gel-state-supported lipid bilayer (SLB).[142] Such SLBs showed uniform coverage around room temperature, while upon heating above their melting temperature and by means of an electrophoresis setup they could originate a gradient of surface-immobilized biomolecules.
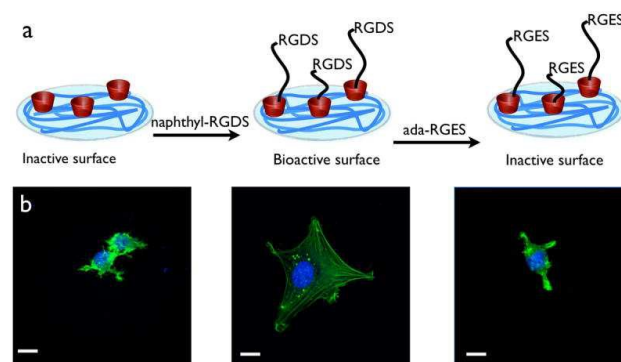

Figure 13. a) Supramolecular host-guest formation between cyclodextrin (red cups) and naphthyl-RGDS renders a surface bioactive. Adamantane-conjugated RGES (ada-RGES) competes with naphthyl-RGDS and makes the surface inactive. b) Confocal microscopy of 3T3 fibroblasts on the inactive surface, the activated surface and the surface with competing ada-RGES present. Scale bars represent 10 μM. Reprinted with permission from reference [140]. Copyright 2014 Wiley-VCH Verlag GmbH & Co.

10 | J. Mater. Chem. B, 2015, 00, 1-3

This journal is © The Royal Society of Chemistry 20xx

Despite these first attempts to design constructs that can function as supramolecular analogues of ECMs, further efforts need to be devoted in engineering synthetic 3D matrices which can efficiently host cell preparations and determine their fate in a spatially defined way. The fundamental advantages of the building mechanisms already proposed on flat surfaces could be adapted to a number of fabrications among the ones we have described in the previous paragraphs.

In addition, already tested platforms, such as bio-printed hydrogels, could be enriched by specific functions that allow host-guest interactions between the support and several complemented cues. From this starting point, the application of sophisticated gradient-forming fabrications (e.g. by employing the gradient maker) or external physical stimuli (e.g. via electrochemistry) could easily enable the formation of supramolecular gradients within the so-designed 3D scaffolds. The combination of supramolecular chemistry and the most advanced scaffold fabrication techniques would introduce the next-generation TE constructs, displaying spatial chemical diversity and tunable characteristics within the same matrix.

Acknowledgements

References

1. A. Seidi, M. Ramalingam, I. Elloumi-Hannachi, S. Ostrovidov and A. Khademhosseini, *Acta Biomater*, 2011, **7**, 1441-1451.
2. J. Genzer, *Ann Rev Mater Res*, 2012, **42**, 435-468.
3. S. B. Carter, *Nature*, 1967, **213**, 256-260.
4. S. V. Plotnikov and C. M. Waterman, *Curr Opin Cell Biol*, 2013, **25**, 619-626.
5. N. Castro, S. A. Hacking and L. Zhang, *Ann Biomed Eng*, 2012, **40**, 1628-1640.
6. S. A. DeLong, A. S. Gobin and J. L. West, *J Control Release*, 2005, **109**, 139-148.
7. S. A. DeLong, J. J. Moon and J. L. West, *Biomaterials*, 2005, **26**, 3227-3234.
8. S. B. Kennedy, N. R. Washburn, C. G. Simon Jr and E. J. Amis, *Biomaterials*, 2006, **27**, 3817-3824.
9. A. J. Engler, S. Sen, H. L. Sweeney and D. E. Discher, *Cell*, 2006, **126**, 677-689.
10. J. M. Sobral, S. G. Caridade, R. A. Sousa, J. F. Mano and R. L. Reis, *Acta Biomater*, 2011, **7**, 1009-1018.
11. S. Morgenthaler, C. Zink and N. D. Spencer, *Soft Matter*, 2008, **4**, 419-434.
12. N. A. Alcantar, E. S. Aydil and J. N. Israelachvili, *J Biomed Mater Res*, 2000, **51**, 343-351.
13. I. Banerjee, R. C. Pangule and R. S. Kane, *Adv Mater*, 2011, **23**, 690-718.
14. A. Jain and S. K. Jain, *Crit Rev Ther Drug Carrier Syst*, 2008, **25**, 403-447.
15. F. M. Veronese and G. Pasut, *Drug Discov Today*, 2005, **10**, 1451-1458.
16. S. Zalipsky, *Adv Drug Deliver Rev*, 1995, **16**, 157-182.
17. J. Zhu, *Biomaterials*, 2010, **31**, 4639-4656.
18. D. W. Hutmacher, *Biomaterials*, 2000, **21**, 2529-2543.
19. S. J. Hollister, *Nat Mater*, 2005, **4**, 518-524.
20. Q. P. Pham, U. Sharma and A. G. Mikos, *Tissue Eng*, 2006, **12**, 1197-1211.
21. K. Rezwan, Q. Z. Chen, J. J. Blaker and A. R. Boccaccini, *Biomaterials*, 2006, **27**, 3413-3431.
22. T. J. Sill and H. A. von Recum, *Biomaterials*, 2008, **29**, 1989-2006.
23. M. K. Chaudhury and G. M. Whitesides, *Science*, 1992, **256**, 1539-1541.
24. R. H. Terrill, K. M. Balss, Y. Zhang and P. W. Bohn, *J Am Chem Soc*, 2000, **122**, 988-989.
25. Q. Wang and P. W. Bohn, *J Phys Chem B*, 2003, **107**, 12578-12584.
26. S. T. Plummer and P. W. Bohn, *Langmuir*, 2002, **18**, 4142-4149.
27. J. C. Love, L. A. Estroff, J. K. Kriebel, R. G. Nuzzo and G. M. Whitesides, *Chem Rev*, 2005, **105**, 1103-1170.
28. S. T. Plummer, Q. Wang, P. W. Bohn, R. Stockton and M. A. Schwartz, *Langmuir*, 2003, **19**, 7528-7536.
29. Q. Wang and P. W. Bohn, *Thin Solid Films*, 2006, **513**, 338-346.
30. V. Corvaglia, R. Marega, F. De Leo, C. Michiels and D. Bonifazi, *Small*, 2016, **12**, 321-329.
31. S. Morgenthaler, S. Lee, S. Zürcher and N. D. Spencer, *Langmuir*, 2003, **19**, 10459-10462.
32. T. Wu, K. Efimenko, P. Vlček, V. Šubr and J. Genzer, *Macromolecules*, 2003, **36**, 2448-2453.
33. S. Edmondson, V. L. Osborne and W. T. S. Huck, *Chem Soc Rev*, 2004, **33**, 14-22.
34. X. Wang, H. Tu, P. V. Braun and P. W. Bohn, *Langmuir*, 2006, **22**, 817-823.
35. R. Barbey, L. Lavanant, D. Paripovic, N. Schuwer, C. Sugnaux, S. Tugulu and H. A. Klok, *Chem. Rev.*, 2009, **109**, 5437-5527.
36. T. Wu, P. Gong, I. Szleifer, P. Vlček, V. Šubr and J. Genzer, *Macromolecules*, 2007, **40**, 8756-8764.
37. P. G. De Gennes, *Macromolecules*, 1980, **13**, 1069-1075.
38. W. J. Brittain and S. Minko, *J. Polym. Sci. Pol. Chem.*, 2007, **45**, 3505-3512.
39. T. Wu, K. Efimenko and J. Genzer, *J Am Chem Soc*, 2002, **124**, 9394-9395.
40. Y. Mei, T. Wu, C. Xu, K. J. Langenbach, J. T. Elliott, B. D. Vogt, K. L. Beers, E. J. Amis and N. R. Washburn, *Langmuir*, 2005, **21**, 12309-12314.
41. Y. Mei, J. T. Elliott, J. R. Smith, K. J. Langenbach, T. Wu, C. Xu, K. L. Beers, E. J. Amis and L. Henderson, *J Biomed Mater Res A*, 2006, **79A**, 974-988.
42. T. Ren, S. Yu, Z. Mao, S. E. Moya, L. Han and C. Gao, *Biomacromolecules*, 2014, **15**, 2256-2264.
43. S. Choi, B. C. Choi, C. Xue and D. Leckband, *Biomacromolecules*, 2013, **14**, 92-100.
44. K. Vasilev, A. Mierczynska, A. L. Hook, J. Chan, N. H. Voelcker and R. D. Short, *Biomaterials*, 2010, **31**, 392-397.
45. J. Wu, Z. Mao and C. Gao, *Biomaterials*, 2012, **33**, 810-820.
46. R. R. Bhat, B. N. Chaney, J. Rowley, A. Liebmann-Vinson and J. Genzer, *Adv Mater*, 2005, **17**, 2802-2807.

This journal is © The Royal Society of Chemistry 20xx

J. Mater. Chem. B, 2015, **00**, 1-3 | **11**

47. M. R. Tomlinson and J. Genzer, *Chem Commun*, 2003, **9**, 1350-1351.

48. L. Li, Y. Zhu, B. Li and C. Gao, *Langmuir*, 2008, **24**, 13632-13639.

49. R. Bhat, M. Tomlinson, T. Wu and J. Genzer, in *Surface-Initiated Polymerization II*, ed. R. Jordan, Springer Berlin Heidelberg, 2006, vol. 198, ch. 60, pp. 51-124.

50. M. R. Tomlinson and J. Genzer, *Macromolecules*, 2003, **36**, 3449-3451.

51. M. Klein Gunnewiek, S. N. Ramakrishna, A. Di Luca, G. J. Vancso, L. Moroni and E. M. Benetti, *Adv Mater Interf*, 2015, DOI: 10.1002/admi.201500456, n/a-n/a.

52. B. Trappmann, J. E. Gautrot, J. T. Connelly, D. G. T. Strange, Y. Li, M. L. Oyen, M. A. Cohen Stuart, H. Boehm, B. Li, V. Vogel, J. P. Spatz, F. M. Watt and W. T. S. Huck, *Nat Mater*, 2012, **11**, 642-649.

53. N. Huebsch, P. R. Arany, A. S. Mao, D. Shvartsman, O. A. Ali, S. A. Bencherif, J. Rivera-Feliciano and D. J. Mooney, *Nat Mater*, 2010, **9**, 518-526.

54. A. P. Kourouklis, R. V. Lerum and H. Bermudez, *Biomaterials*, 2014, **35**, 4827-4834.

55. S. Tugulu, P. Silacci, N. Stergiopulos and H.-A. Klok, *Biomaterials*, 2007, **28**, 2536-2546.

56. S. Morgenthaler, C. Zink, B. Städler, J. Vörös, S. Lee, N. D. Spencer and S. G. P. Tosatti, *Biointerphases*, 2006, **1**, 156-165.

57. J. Pei, H. Hall and N. D. Spencer, *Biomaterials*, 2011, **32**, 8968-8978.

58. A. Halperin, *Langmuir*, 1999, **15**, 2525-2533.

59. M. Müller, S. Lee, H. Spikes and N. Spencer, *Tribol Lett*, 2003, **15**, 395-405.

60. J. W. Lussi, D. Falconnet, J. A. Hubbell, M. Textor and G. Csucs, *Biomaterials*, 2006, **27**, 2534-2541.

61. M. Jaspers, M. Dennison, M. F. J. Mabesoone, F. C. MacKintosh, A. E. Rowan and P. H. J. Kouwer, *Nat Commun*, 2014, **5**.

62. S. T. K. Raja, T. Thiruselvi, A. B. Mandal and A. Gnanamani, *Sci Rep*, 2015, **5**, 15977.

63. I. Caelen, A. Bernard, D. Juncker, B. Michel, H. Heinzelmann and E. Delamarche, *Langmuir*, 2000, **16**, 9125-9130.

64. N. L. Jeon, S. K. W. Dertinger, D. T. Chiu, I. S. Choi, A. D. Stroock and G. M. Whitesides, *Langmuir*, 2000, **16**, 8311-8316.

65. R. C. Gunawan, E. R. Choban, J. E. Conour, J. Silvestre, L. B. Schook, H. R. Gaskins, D. E. Leckband and P. J. A. Kenis, *Langmuir*, 2005, **21**, 3061-3068.

66. S. Kim, H. J. Kim and N. L. Jeon, *Integr Biol*, 2010, **2**, 584-603.

67. A. G. Toh, Z. P. Wang, C. Yang and N.-T. Nguyen, *Microfluid Nanofluid*, 2014, **16**, 1-18.

68. K. A. Fosser and R. G. Nuzzo, *Anal Chem*, 2003, **75**, 5775-5782.

69. J. He, Y. Du, J. L. Villa-Uribe, C. Hwang, D. Li and A. Khademhosseini, *Adv Funct Mater*, 2010, **20**, 131-137.

70. J. A. Burdick, A. Khademhosseini and R. Langer, *Langmuir*, 2004, **20**, 5153-5156.

71. X. Jiang, Q. Xu, S. K. W. Dertinger, A. D. Stroock, T.-m. Fu and G. M. Whitesides, *Anal Chem*, 2005, **77**, 2338-2347.

72. R. C. Gunawan, J. Silvestre, H. R. Gaskins, P. J. A. Kenis and D. E. Leckband, *Langmuir*, 2006, **22**, 4250-4258.

73. S. Allazetta, S. Cosson and M. P. Lutolf, *Chem Commun*, 2011, **47**, 191-193.

74. S. Cosson, S. Allazetta and M. P. Lutolf, *Lab Chip*, 2013, **13**, 2099-2105.

75. S. Cosson, S. A. Kobel and M. P. Lutolf, *Adv Funct Mater*, 2009, **19**, 3411-3419.

76. D. H. Reneker and A. L. Yarin, *Polymer*, 2008, **49**, 2387-2425.

77. Handarmin, G. J. Y. Tan, B. Sundaray, G. T. Marcy, E. L. K. Goh and S. Y. Chew, *Drug Deliv. and Transl. Res.*, 2011, **1**, 147-160.

78. X. Zhang, X. Gao, L. Jiang and J. Qin, *Langmuir*, 2012, **28**, 10026-10032.

79. H. G. Sundararaghavan and J. A. Burdick, *Biomacromolecules*, 2011, **12**, 2344-2350.

80. S. Samavedi, C. Olsen Horton, S. A. Guelcher, A. S. Goldstein and A. R. Whittington, *Acta Biomater*, 2011, **7**, 4131-4138.

81. W. Bonani, D. Maniglio, A. Motta, W. Tan and C. Migliaresi, *J Biomed Mater Res B*, 2011, **96B**, 276-286.

82. S. Samavedi, S. A. Guelcher, A. S. Goldstein and A. R. Whittington, *Biomaterials*, 2012, **33**, 7727-7735.

83. W. Bonani, A. Motta, C. Migliaresi and W. Tan, *Langmuir*, 2012, **28**, 13675-13687.

84. F. Du, H. Wang, W. Zhao, D. Li, D. Kong, J. Yang and Y. Zhang, *Biomaterials*, 2012, **33**, 762-770.

85. X. Guo, C. G. Elliott, Z. Li, Y. Xu, D. W. Hamilton and J. Guan, *Biomacromolecules*, 2012, **13**, 3262-3271.

86. X. Li, J. Xie, J. Lipner, X. Yuan, S. Thomopoulos and Y. Xia, *Nano Lett*, 2009, **9**, 2763-2768.

87. J. Shi, L. Wang, F. Zhang, H. Li, L. Lei, L. Liu and Y. Chen, *ACS Appl Mater Interfaces*, 2010, **2**, 1025-1030.

88. B. Zou, Y. Liu, X. Luo, F. Chen, X. Guo and X. Li, *Acta Biomater*, 2012, **8**, 1576-1585.

89. H. K. Min, S. H. Oh, J. M. Lee, G. I. Im and J. H. Lee, *Acta Biomater*, 2014, **10**, 1272-1279.

90. S. H. Oh, J. H. Kim, J. M. Kim and J. H. Lee, *J Biomater Sci Polym Ed*, 2006, **17**, 1375-1387.

91. S. H. Oh, I. K. Park, J. M. Kim and J. H. Lee, *Biomaterials*, 2007, **28**, 1664-1671.

92. S. H. Oh, T. H. Kim, G. I. Im and J. H. Lee, *Biomacromolecules*, 2010, **11**, 1948-1955.

93. T. Kim, S. Oh, E. Kwon, J. Lee and J. Lee, *Macromol. Res.*, 2013, **21**, 878-885.

94. S. H. Oh, T. H. Kim and J. H. Lee, *Biomaterials*, 2011, **32**, 8254-8260.

95. L. Moroni, J. R. de Wijn and C. A. van Blitterswijk, *J Biomed Mater Res A*, 2005, **75A**, 957-965.

96. L. Moroni, J. R. de Wijn and C. A. van Blitterswijk, *Biomaterials*, 2006, **27**, 974-985.

97. M. Klein Gunnewiek, A. Di Luca, H. Z. Bollemaat, C. A. van Blitterswijk, G. J. Vancso, L. Moroni and E. M. Benetti, *Adv Healthc Mater*, 2015, **4**, 1169-1174.

98. K. Chatterjee, S. Lin-Gibson, W. E. Wallace, S. H. Parekh, Y. J. Lee, M. T. Cicerone, M. F. Young and C. G. Simon Jr, *Biomaterials*, 2010, **31**, 5051-5062.

99. S. Nemir, H. N. Hayenga and J. L. West, *Biotechnol Bioeng*, 2010, **105**, 636-644.

100. X. Wang, E. Wenk, X. Zhang, L. Meinel, G. Vunjak-Novakovic and D. L. Kaplan, *J Control Release*, 2009, **134**, 81-90.

12 | *J. Mater. Chem. B*, 2015, **00**, 1-3

This journal is © The Royal Society of Chemistry 20xx

101. D. Guarnieri, A. De Capua, M. Ventre, A. Borzacchiello, C. Pedone, D. Marasco, M. Ruvo and P. A. Netti, *Acta Biomater*, 2010, **6**, 2532-2539.
102. L. A. Smith Callahan, E. P. Childers, S. L. Bernard, S. D. Weiner and M. L. Becker, *Acta Biomater*, 2013, **9**, 7420-7428.
103. L. A. Smith Callahan, A. M. Ganios, E. P. Childers, S. D. Weiner and M. L. Becker, *Acta Biomater*, 2013, **9**, 6095-6104.
104. L. A. Smith Callahan, G. M. Policastro, S. L. Bernard, E. P. Childers, R. Boettcher and M. L. Becker, *Biomacromolecules*, 2013, **14**, 3047-3054.
105. A. Sala, P. Hanseler, A. Ranga, M. P. Lutolf, J. Vörös, M. Ehrbar and F. E. Weber, *Integr Biol*, 2011, **3**, 1102-1111.
106. M. S. Hahn, J. S. Miller and J. L. West, *Adv Mater*, 2005, **17**, 2939-2942.
107. M. S. Hahn, J. S. Miller and J. L. West, *Adv Mater*, 2006, **18**, 2679-2684.
108. M. S. Hahn, L. J. Taite, J. J. Moon, M. C. Rowland, K. A. Ruffino and J. L. West, *Biomaterials*, 2006, **27**, 2519-2524.
109. J. C. Hoffmann and J. L. West, *Soft Matter*, 2010, **6**, 5056-5063.
110. B. D. Polizzotti, B. D. Fairbanks and K. S. Anseth, *Biomacromolecules*, 2008, **9**, 1084-1087.
111. C. A. DeForest and K. S. Anseth, *Nat Chem*, 2011, **3**, 925-931.
112. C. A. DeForest and K. S. Anseth, *Angew Chem Int Ed*, 2012, **51**, 1816-1819.
113. K. A. Mosiewicz, L. Kolb, A. J. van der Vlies, M. M. Martino, P. S. Lienemann, J. A. Hubbell, M. Ehrbar and M. P. Lutolf, *Nat Mater*, 2013, **12**, 1072-1078.
114. R. G. Wylie, S. Ahsan, Y. Aizawa, K. L. Maxwell, C. M. Morshead and M. S. Shoichet, *Nat Mater*, 2011, **10**, 799-806.
115. R. G. Wylie and M. S. Shoichet, *Biomacromolecules*, 2011, **12**, 3789-3796.
116. S. Khetan and J. A. Burdick, *Soft Matter*, 2011, **7**, 830-838.
117. V. Milleret, B. R. Simona, P. S. Lienemann, J. Vörös and M. Ehrbar, *Adv Healthc Mater*, 2014, **3**, 508-514.
118. E. Cukierman, R. Pankov and K. M. Yamada, *Curr Opin Cell Biol*, 2002, **14**, 633-640.
119. M. A. Wozniak, K. Modzelewska, L. Kwong and P. J. Keely, *BBA-Mol Cell Res*, 2004, **1692**, 103-119.
120. S. I. Fraley, Y. Feng, R. Krishnamurthy, D.-H. Kim, A. Celedon, G. D. Longmore and D. Wirtz, *Nat Cell Biol*, 2010, **12**, 598-604.
121. B. Geiger, J. P. Spatz and A. D. Bershadsky, *Nat Rev Mol Cell Bio*, 2009, **10**, 21-33.
122. M. Prager-Khoutorsky, A. Lichtenstein, R. Krishnan, K. Rajendran, A. Mayo, Z. Kam, B. Geiger and A. D. Bershadsky, *Nat Cell Biol*, 2011, **13**, 1457-1465.
123. S. I. Fraley, Y. Feng, R. Krishnamurthy, D. H. Kim, A. Celedon, G. D. Longmore and D. Wirtz, *Nat Cell Biol*, 2010, **12**, 598-604.
124. E. A. Cavalcanti-Adam, A. Micoulet, J. Blümmel, J. Auernheimer, H. Kessler and J. P. Spatz, *Eur J Cell Biol*, 2006, **85**, 219-224.
125. E. A. Cavalcanti-Adam, T. Volberg, A. Micoulet, H. Kessler, B. Geiger and J. P. Spatz, *Biophys J*, 2007, **92**, 2964-2974.
126. P. A. Underwood and F. A. Bennett, *J Cell Sci*, 1989, **93**, 641-649.
127. Y. N. Danilov and R. L. Juliano, *Exp Cell Res*, 1989, **182**, 186-196.
128. B. K. Brandley and R. L. Schnaar, *Dev Biol*, 1989, **135**, 74-86.
129. E. M. Levine, H. Roelink, J. Turner and T. A. Reh, *J Neurosci*, 1997, **17**, 6277-6288.
130. M. Fu, V. C. H. Lui, M. H. Sham, V. Pachnis and P. K. H. Tam, *J Cell Biol*, 2004, **166**, 673-684.
131. E. Angot, K. Loulier, K. T. Nguyen-Ba-Charvet, A. P. Gadeau, M. Ruat and E. Traiffort, *Stem Cells*, 2008, **26**, 2311-2320.
132. E. Cukierman, R. Pankov, D. R. Stevens and K. M. Yamada, *Science*, 2001, **294**, 1708-1712.
133. R. J. Petrie, N. Gavara, R. S. Chadwick and K. M. Yamada, *J Cell Biol*, 2012, **197**, 439-455.
134. S. Even-Ram and K. M. Yamada, *Curr Opin Cell Biol*, 2005, **17**, 524-532.
135. K. A. Kyburz and K. S. Anseth, *Acta Biomater*, 2013, **9**, 6381-6392.
136. P. C. Bessa, M. Casal and R. L. Reis, *J Tissue Eng Regen M*, 2008, **2**, 81-96.
137. R. McBeath, D. M. Pirone, C. M. Nelson, K. Bhadriraju and C. S. Chen, *Dev Cell*, 2004, **6**, 483-495.
138. S. Dupont, L. Morsut, M. Aragona, E. Enzo, S. Giulitti, M. Cordenonsi, F. Zanconato, J. Le Digabel, M. Forcato, S. Bicciato, N. Elvassore and S. Piccolo, *Nature*, 2011, **474**, 179-183.
139. H.-J. Schneider, *Angew Chem Int Ed*, 2009, **48**, 3924-3977.
140. J. Boekhoven and S. I. Stupp, *Adv Mater*, 2014, **26**, 1642-1659.
141. H. Yang, B. Yuan, X. Zhang and O. A. Scherman, *Accounts Chem Res*, 2014, **47**, 2106-2115.
142. J. Cabanas-Danés, E. D. Rodrigues, E. Landman, J. van Weerd, C. van Blitterswijk, T. Verrips, J. Huskens, M. Karperien and P. Jonkheijm, *J Am Chem Soc*, 2014, **136**, 12675-12681.

This journal is © The Royal Society of Chemistry 20xx

J. Mater. Chem. B, 2015, **00**, 1-3 | **13**